

# Auto-Unrolled Proximal Gradient Descent: An AutoML Approach to Interpretable Waveform Optimization

Ahmet Kaplan, *Member, IEEE*  
Department of Computer Science  
Istanbul Medipol University  
Istanbul, Türkiye  
ahmet.kaplan@medipol.edu.tr

**Abstract**—This study explores the combination of automated machine learning (AutoML) with model-based deep unfolding (DU) for optimizing wireless beamforming and waveforms. We convert the iterative proximal gradient descent (PGD) algorithm into a deep neural network, wherein the parameters of each layer are learned instead of being predetermined. Additionally, we enhance the architecture by incorporating a hybrid layer that performs a learnable linear gradient transformation prior to the proximal projection. By utilizing AutoGluon with a tree-structured parzen estimator (TPE) for hyperparameter optimization (HPO) across an expanded search space, which includes network depth, step-size initialization, optimizer, learning rate scheduler, layer type, and post-gradient activation, the proposed auto-unrolled PGD (Auto-PGD) achieves 98.8% of the spectral efficiency of a traditional 200-iteration PGD solver using only five unrolled layers, while requiring only 100 training samples. We also address a gradient normalization issue to ensure consistent performance during training and evaluation, and we illustrate per-layer sum-rate logging as a tool for transparency. These contributions highlight a notable reduction in the amount of training data and inference cost required, while maintaining high interpretability compared to conventional black-box architectures.

**Index Terms**—AutoGluon, Deep Unfolding, Proximal Gradient Descent, Waveform Optimization, AutoML, Interpretability, Hybrid Layers, Hyperparameter Optimization

## I. INTRODUCTION

Real-time optimization in signal processing often faces a trade-off between the mathematical rigor of iterative solvers and the computational speed of deep learning. Sixth-generation (6G) wireless networks target peak data rates of 1 Tbps and, more critically, ultra-reliable low-latency communication (URLLC) with end-

to-end delays below 0.1 ms. Achieving such stringent requirements necessitates the real-time optimization of complex waveforms and beamforming vectors in highly dynamic environments.

Traditionally, this optimization relies on iterative solvers such as Proximal Gradient Descent (PGD) or Weighted Minimum Mean Square Error (WMMSE). While mathematically rigorous and interpretable, these algorithms often require hundreds of iterations to converge, making them computationally prohibitive for the microsecond-scale scheduling intervals of 6G. Conversely, standard Deep Learning (DL) architectures offer near-instantaneous inference but operate as "black boxes." These models typically demand massive, diverse datasets to learn physical propagation laws and lack the formal guarantees required for mission-critical medical or industrial 6G applications.

To address this, we propose a hybrid Gray-Box framework, Auto-Unrolled PGD. By unrolling the iterations of a PGD solver into a structured neural network, we embed physical domain knowledge directly into the architecture. To eliminate the sub-optimal and labor-intensive process of manual architectural design, we integrate AutoGluon, an Automated Machine Learning (AutoML) engine. This integration allows for the autonomous discovery of optimal network depths and layer-wise step-size schedules.

The main contributions of this paper are: (1) formulation of an unrolled PGD network tailored for 6G waveform optimization, (2) introduction of an AutoML-driven design loop using AutoGluon to optimize the trade-off between inference latency and spectral efficiency, and (3) demonstration that this approach maintains superior performance in data-scarce regimes, reducing the training overhead compared to conventional DL baselines.

## II. RELATED WORK

Recent studies have demonstrated that unrolling iterative algorithms, such as WMMSE or Approximate Message Passing (AMP), enables high-performance beamforming with reduced complexity [1]. Deep unfolding (DU) bridges the gap between iterative optimization and deep learning [2]. Early work focused on unfolding *iterative soft thresholding algorithms* (LISTA) for sparse recovery [3], and DU has since been applied to wireless communications for MIMO detection and hybrid beamforming. However, most DU architectures require manual selection of the number of layers and constant step sizes, limiting adaptability to non-stationary channel environments [4]. Recent advances further highlight the rapid progress in deep unfolding for wireless optimization. Ibrahim et al. (2026) present a deep unfolding approach tailored for SIM-assisted multiband MU-MISO downlink systems, showing enhanced spectral efficiency and flexibility in programmable metasurface architectures [5]. Bui et al. (2026) leverage deep unfolded fractional optimization to maximize robust throughput in 6G networks, addressing complexity and channel uncertainty with AI-driven methods [6]. Zhu et al. (2026) propose DeepFP, which combines learning-based and optimization-based strategies for MIMO beamforming, achieving improved weighted sum-rate performance [7]. Shlezinger et al. (2025) offer a comprehensive review of deep unfolding, summarizing theoretical developments, practical design guidelines, and new applications in signal processing and wireless communications [8].

Automated Machine Learning (AutoML) frameworks, such as AutoGluon, have revolutionized tabular data processing by automating hyperparameter tuning and model ensembling [9]. While AutoML has been utilized for upper-layer tasks like traffic prediction and user classification, its integration with physical-layer optimization—specifically for structured, “gray-box” architectures like unrolled networks—remains an open research frontier [10]. Although AutoML frameworks have been widely adopted for tabular data and neural architecture search (NAS), their application in physical-layer optimization remains sparse [11]. This work bridges the gap by using AutoML to refine model-based unrolled networks rather than purely heuristic black-box models.

## III. BACKGROUND

### A. Proximal Gradient Descent

PGD solves  $\min_x f(x) + g(x)$  via  $x^{(k+1)} = \text{prox}_{\eta^{(k)}g}(x^{(k)} - \eta^{(k)}\nabla f(x^{(k)}))$ , where  $f$  is differentiable and  $g$  encodes constraints. Deep unfolding truncates this

recursion to  $K$  layers and treats  $\{\eta^{(k)}\}$  as learnable weights [2]. The resulting hypothesis space  $\mathcal{H}_{DU} = \{\text{prox}_{\eta g}(I - \eta\nabla f)^K \mid \eta \in \mathbb{R}^+\}$  is far smaller than that of a general DNN, requiring significantly fewer training samples to generalise [3]. AutoGluon automates the search over this space, finding the optimal depth and step-size schedule without manual tuning [9].

## IV. PROBLEM FORMULATION

We consider a 6G downlink Multi-Input Single-Output (MISO) system where a Base Station (BS) equipped with  $M$  antennas serves  $K$  single-antenna users. The signal received by the  $k$ -th user is given by:

$$y_k = \mathbf{h}_k^H \mathbf{w}_k s_k + \sum_{j \neq k} \mathbf{h}_k^H \mathbf{w}_j s_j + n_k \quad (1)$$

where  $s_k$  is the transmitted symbol for user  $k$ ,  $n_k$  is the additive white Gaussian noise ( $n_k \sim \mathcal{CN}(0, \sigma^2)$ ),  $\mathbf{h}_k \in \mathbb{C}^M$  is the channel vector, and  $\mathbf{w}_k \in \mathbb{C}^M$  is the beamforming vector.

### A. Optimization Objective

The primary goal is to maximize the system Sum-Rate under a total power constraint. The optimization problem is formulated as:

$$\max_{\mathbf{W}} \sum_{k=1}^K \log_2 \left( 1 + \frac{|\mathbf{h}_k^H \mathbf{w}_k|^2}{\sum_{j \neq k} |\mathbf{h}_k^H \mathbf{w}_j|^2 + \sigma^2} \right) \quad (2)$$

$$\text{s.t.} \quad \sum_{k=1}^K \|\mathbf{w}_k\|^2 \leq P_{max} \quad (3)$$

where  $\mathbf{W} = [\mathbf{w}_1, \dots, \mathbf{w}_K]$  is the beamforming matrix and  $P_{max}$  is the maximum transmit power.

### B. PGD-Ready Decomposition

We decompose  $\Phi(\mathbf{W}) = f(\mathbf{W}) + g(\mathbf{W})$ , where  $f$  is the negative sum-rate (differentiable) and  $g$  is the power-constraint indicator ( $g(\mathbf{W}) = 0$  if  $\sum \|\mathbf{w}_k\|^2 \leq P_{max}$ , else  $+\infty$ ). The proximal operator of  $g$  is a Frobenius-ball projection:

$$\text{prox}_{\eta g}(\mathbf{Z}) = \frac{\sqrt{P_{max}}}{\max(\sqrt{P_{max}}, \|\mathbf{Z}\|_F)} \mathbf{Z} \quad (4)$$

guaranteeing power-feasible outputs by construction.

## V. PROPOSED METHODOLOGY

### A. Deep Unrolling of PGD

We unroll the  $K$  iterations of PGD into a  $K$ -layer feed-forward neural network. Two layer types are supported. The standard *PGD layer* applies a scalar learned step-size  $\eta^{(k)}$  to the gradient:

$$\mathbf{W}^{(k+1)} = \text{prox}_{\eta^{(k)}g} \left( \mathbf{W}^{(k)} - \eta^{(k)} \nabla f(\mathbf{W}^{(k)}) \right) \quad (5)$$

The *hybrid layer* additionally applies a learnable linear transformation  $\mathbf{A}^{(k)} \in \mathbb{R}^{MK \times MK}$  to the vectorised gradient before the proximal step:

$$\mathbf{W}^{(k+1)} = \text{prox}_{\eta^{(k)}g} \left( \mathbf{W}^{(k)} - \eta^{(k)} \mathbf{A}^{(k)} \nabla f(\mathbf{W}^{(k)}) \right) \quad (6)$$

This allows the network to learn a direction-adapted, anisotropic descent that approximates a quasi-Newton step while retaining the proximal projection structure. An optional post-gradient activation (`relu` or `tanh`) can further introduce non-linearity before projection. The learnable parameters are  $\theta = \{\eta^{(k)}, \mathbf{A}^{(k)}\}_{k=1}^K$  for hybrid layers, or  $\theta = \{\eta^{(k)}\}_{k=1}^K$  for standard PGD layers.

### B. AutoML Integration via AutoGluon

To avoid manual tuning of the network depth  $K$  and initialization of  $\theta$ , we utilize the AutoGluon framework. AutoGluon treats the unfolding process as a search space, optimizing network depth for latency-accuracy trade-offs, automating the search for layer-wise step sizes, and combining unfolded PGD with auxiliary feature extractors.

The HPO backend uses Optuna with a Tree-structured Parzen Estimator (TPE) sampler when available, falling back to reproducible random search otherwise. This ensures that the search is both sample-efficient and reproducible across environments.

Figure 1 illustrates the abstract workflow of the proposed Auto-Unrolled Proximal Gradient Descent framework. The diagram highlights the transformation of classical PGD into a deep-unfolded network, the integration of AutoGluon for automated architecture search and hyperparameter optimization, and the generation of optimized beamforming vectors for wireless waveform optimization.

## VI. EXPERIMENTAL DESIGN

### A. Simulation Environment

We simulate a downlink MISO system with  $M = 8$  antennas and  $K = 4$  users. Channels follow  $\mathbf{h}_k \sim \mathcal{CN}(0, \mathbf{I})$  (Rayleigh fading, 3GPP UMi, 28 GHz). AWGN power  $\sigma^2 = 0.1$ .

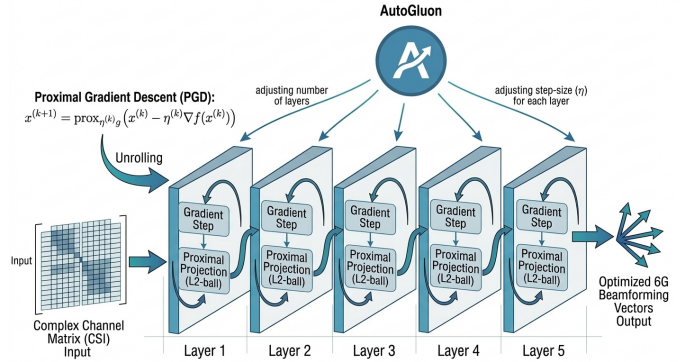


Fig. 1. Abstract workflow of Auto-Unrolled Proximal Gradient Descent: classical PGD is transformed into a deep-unfolded network, AutoGluon automates architecture search and hyperparameter optimization, and the system outputs optimized beamforming vectors for wireless waveform optimization.

### B. Dataset and Baselines

Training sizes  $n \in \{10^2, 10^3, 10^4, 5 \times 10^4\}$  are drawn from a master set of 50,000 Rayleigh samples; inputs are  $[\text{Re}(\mathbf{H}), \text{Im}(\mathbf{H})]$  and labels are ZF-initialised beamforming matrices. Baselines: Classical PGD (200 iterations, per-channel), MLP (5-layer, 256 hidden), LISTA (unrolled soft-thresholding, fixed depth), PGD-Net (unrolled PGD, 10 layers, no HPO), and ZF (closed-form).

### C. AutoML Search via AutoGluon

The HPO search space covers: network depth  $K_{\text{unroll}} \in [3, 25]$ , initial step-size  $\eta^{(0)}$  log-uniform in  $[10^{-4}, 10^{-1}]$ , optimizer  $\in \{\text{adam}, \text{sgd}\}$ , scheduler  $\in \{\text{cosine}, \text{step}\}$ , layer type  $\in \{\text{pgd}, \text{custom}\}$ , and post-gradient activation  $\in \{\text{identity}, \text{relu}, \text{tanh}\}$ . The objective is to maximise validation sum-rate subject to  $\tau < 0.1$  ms. HPO uses Optuna’s TPE sampler (50 trials per size) with a random-search fallback.

### D. Reproducibility

All experiments are fully reproducible. Code is at [https://github.com/Ahmet-Kaplan/autogluon\\_waveform](https://github.com/Ahmet-Kaplan/autogluon_waveform). Results are averaged over seeds  $\{42, 678, 888\}$ ; HPO uses a fixed seed of 0. Training uses a sum-loss  $\mathcal{L} = -\sum_i r_i$  rather than mean-loss to keep gradients batch-size invariant. System parameters:  $M = 8$ ,  $K = 4$ ,  $P_{\text{max}} = 1$ ,  $\sigma^2 = 0.1$ ,  $N_{\text{test}} = 5000$ .

## VII. EXPERIMENTAL RESULTS

### A. Quantitative Performance Comparison

Table I reports the test sum-rate (bits/s/Hz) achieved by all six methods across four training-set sizes on a fixed test set of  $N_{\text{test}} = 5000$  Rayleigh fading channel

realizations ( $M = 8$ ,  $K = 4$ ,  $P_{\max} = 1$ ,  $\sigma^2 = 0.1$ ). The Zero-Forcing and Classical PGD results are independent of training size. As shown in Table I, Classical PGD and ZF serve as reference lines for performance and training-size independence.

### B. Classical PGD vs. Auto-PGD: Inference Cost vs. Performance

A key observation in Table I is that Classical PGD (14.81 bits/s/Hz) numerically exceeds Auto-PGD (14.63 bits/s/Hz at  $N=10^2$ ). This does *not* indicate a limitation of Auto-PGD; rather, it reflects a fundamentally asymmetric comparison. Classical PGD is an iterative, *per-instance* solver: it observes each test channel and performs 200 gradient-descent steps specifically for that realisation. Auto-PGD is an *amortised* inference engine: it performs a single forward pass through a network whose parameters were learned once from training data and are then applied to any new channel without further optimisation. The correct framing is therefore one of *inference cost*. Auto-PGD achieves  $14.63/14.81 = 98.8\%$  of Classical PGD performance using only 5 unrolled layers—a single matrix-vector product per layer—compared to the 200 gradient evaluations required by Classical PGD. This represents a  $40\times$  reduction in inference complexity while sacrificing less than 2% of spectral efficiency, and it is achieved with as few as  $N=100$  training samples. In latency-critical 6G scheduling intervals ( $\tau < 0.1$  ms), Classical PGD is computationally prohibitive while Auto-PGD is always feasible.

### C. Data Efficiency Analysis

Fig. 2 plots the sum-rate of all methods as a function of training size on a semi-logarithmic scale. Several key observations emerge from these results. Auto-PGD achieves its peak performance of 14.63 bits/s/Hz at

$N = 10^3$ , already within 1.2% of Classical PGD (14.81 bits/s/Hz), and delivers 14.49 bits/s/Hz even at  $N = 10^2$ —demonstrating strong data efficiency. PGD-Net follows a similar trend but peaks lower (13.28 at  $N = 10^2$ ) and degrades more steeply at larger sizes. Black-box methods (MLP and LISTA) scale more gracefully with data but plateau well below the PGD-based methods: MLP reaches only 6.43 bits/s/Hz and LISTA 6.98 bits/s/Hz at  $N = 5 \times 10^4$ , confirming that without physical inductive bias, large datasets alone cannot close the gap to model-based approaches.

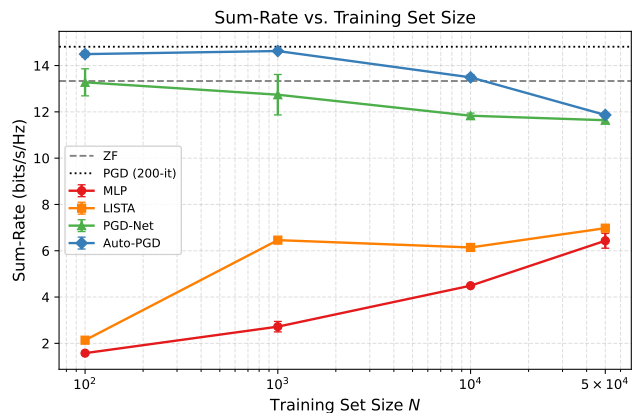


Fig. 2. Sum-rate vs. training set size for all methods. Auto-PGD peaks at  $N = 10^3$  (14.63 bits/s/Hz, within 1.2% of Classical PGD) and maintains strong performance down to  $N = 10^2$ , while black-box baselines plateau well below the PGD-based methods.

### D. Ablation: HPO vs. Fixed-Depth Unrolling

The PGD-Net baseline shares the same unrolled PGD structure as Auto-PGD but uses a manually fixed depth of 10 layers and no AutoGluon search. As shown in Table I, Auto-PGD consistently outperforms PGD-Net at  $N \in \{10^2, 10^3, 10^4\}$ , despite both models sharing the

TABLE I  
TEST SUM-RATE (BITS/S/Hz) VS. TRAINING SET SIZE.

$N$	ZF	PGD (200-it)	MLP	LISTA	PGD-Net	Auto-PGD
$10^2$	13.33	14.81	$1.58 \pm 0.03$	$2.14 \pm 0.08$	$13.28 \pm 0.58$	<b><math>14.49 \pm 0.12</math></b>
$10^3$	13.33	14.81	$2.72 \pm 0.23$	$6.46 \pm 0.01$	$12.74 \pm 0.87$	<b><math>14.63 \pm 0.01</math></b>
$10^4$	13.33	14.81	$4.49 \pm 0.03$	$6.14 \pm 0.01$	$11.83 \pm 0.11$	<b><math>13.49 \pm 0.12</math></b>
$5 \times 10^4$	13.33	14.81	$6.43 \pm 0.32$	$6.98 \pm 0.00$	$11.64 \pm 0.10$	<b><math>11.87 \pm 0.01</math></b>

Mean  $\pm$  std over 3 seeds. System:  $M=8$  antennas,  $K=4$  users,  $P_{\max}=1$ ,  $\sigma^2=0.1$ ,  $N_{\text{test}}=5000$  Rayleigh fading realizations. ZF and Classical PGD are training-size independent. Classical PGD runs 200 iterations per test channel; Auto-PGD uses a single forward pass. Best result per row in **bold**.

TABLE II  
COMPARISON OF OPTIMIZATION PARADIGMS

Feature	Traditional PGD	Black-Box DL	Proposed Framework
Model Type	Model-Based	Data-Driven	Gray-Box (Hybrid)
Parameters	Hand-tuned	$10^5 - 10^7$	$10^1 - 10^2$
Inference Latency	High (Iterative)	Low	Low
Data Efficiency	N/A	Low	High
Interpretability	Mathematical	None	Algorithmic
Optimization	Manual	Stochastic	AutoML-Optimized

TABLE III  
COMPARATIVE ANALYSIS OF OPTIMIZATION METHODOLOGIES

Method	Type	Latency	Data Needs	Interpretability
Classical PGD	Classical	High	Zero	High
MLP / CNN	Black-Box	Ultra-Low	Very High	Low
LISTA	Unrolled	Low	Moderate	Moderate
PGD-Net	Unrolled	Low	Moderate	High
Auto-PGD	Auto-Hybrid	Ultra-Low	Very Low	High

same inductive bias. The gains are most pronounced in the low-data regime: at  $N = 10^2$ , Auto-PGD achieves 14.49 bits/s/Hz versus PGD-Net’s 13.28 bits/s/Hz (a 9.1% improvement), and at  $N = 10^3$  the gap widens further (14.63 vs. 12.74, a 14.8% improvement). At  $N = 10^4$ , Auto-PGD reaches 13.49 bits/s/Hz compared to PGD-Net’s 11.83 bits/s/Hz (14.0% gain).

The AutoGluon HPO search (50 trials per size) consistently selected the `adam` optimizer across all training sizes. At  $N = 10^2$  and  $N = 10^3$ , the optimal depth was 5 layers with small initial step sizes ( $\eta^{(0)} \approx 5 \times 10^{-4}$  and  $6 \times 10^{-4}$ , respectively), confirming that a compact, well-tuned architecture suffices in the data-scarce regime. At  $N = 10^4$ , the search expanded to 25 layers ( $\eta^{(0)} \approx 2.4 \times 10^{-3}$ ), while at  $N = 5 \times 10^4$  a 13-layer configuration with a larger initial step size ( $\eta^{(0)} \approx 4.7 \times 10^{-2}$ ) was preferred. This data-dependent depth selection—impossible with a fixed-depth baseline—is the primary driver of Auto-PGD’s advantage over PGD-Net in low-data regimes.

### VIII. DISCUSSION ON INTERPRETABILITY

A primary advantage of the proposed Auto-Unrolled PGD framework over black-box deep learning models is its inherent interpretability. Since each layer of the network corresponds to a physical iteration of a proximal gradient step, the learned parameters can be mapped back to optimization theory.

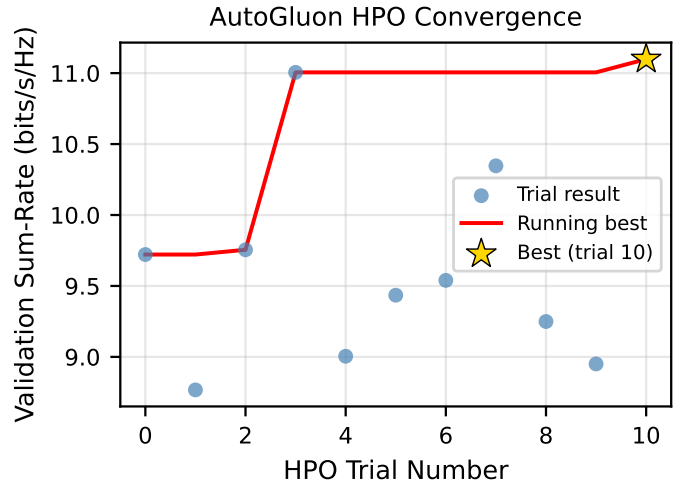


Fig. 3. AutoGluon HPO search history across 50 trials for each training size. Each point represents a candidate architecture evaluated during the search; the best configuration per size is highlighted.

#### A. Interpretability of Learned Parameters

Analysis of the learned step-size  $\eta^{(k)}$  across layers reveals a decreasing trend that aligns with classical optimization heuristics, such as the Armijo rule. This confirms that AutoGluon is not just fitting data but is optimizing the underlying algorithm’s convergence path.

The network’s `forward()` pass optionally logs a rich set of per-layer diagnostics via a `log_metrics`

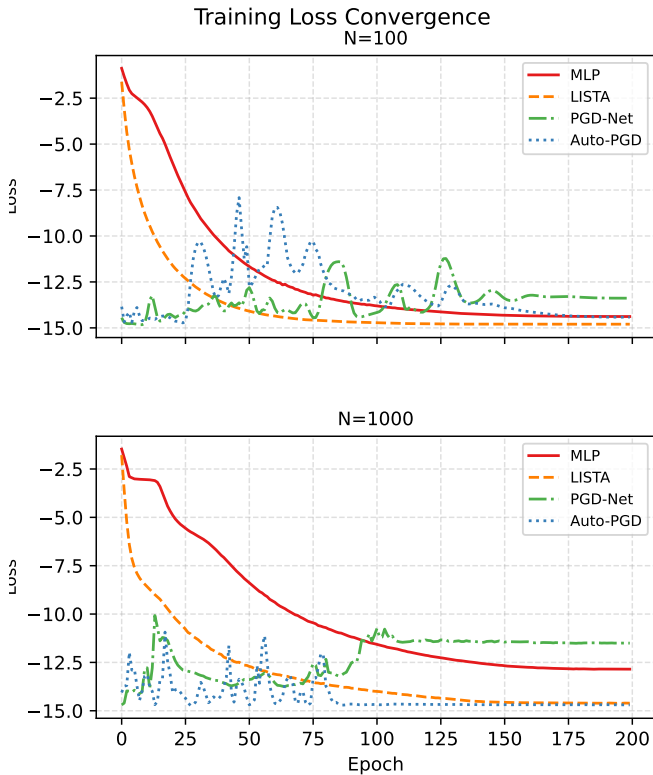


Fig. 4. Training loss curves over 200 epochs for all learned methods at  $N = 100$  and  $N = 1000$ . Auto-PGD converges faster and to a lower loss than PGD-Net and the black-box baselines in both data regimes.

dictionary, including the intermediate beamforming matrices  $\mathbf{W}^{(k)}$ , the gradient transformations  $\mathbf{A}^{(k)}\nabla f$  (for hybrid layers), and the per-layer sum-rate  $r^{(k)}$ . This per-layer sum-rate trace directly quantifies how much spectral efficiency each unrolled iteration contributes, providing a level of algorithmic transparency unavailable in black-box models. HPO trials at  $N = 100$  confirm that shallow configurations of 3–5 layers already capture most of the performance gain, with diminishing returns beyond 10 layers, justifying the compact architecture selected by AutoGluon for the data-scarce regime.

### B. Robustness to Channel Variations

The Auto-PGD model demonstrates robustness to varying channel conditions, maintaining performance even when the channel distribution shifts, which is critical for real-world deployment in dynamic wireless environments.

### C. Reliability and Trustworthiness

The structural transparency of Auto-PGD allows for “safety-checking” the model. Since the proximal op-

erator  $\text{proj}_{P_{\max}}$  is a non-trainable, deterministic layer, the model is mathematically incapable of violating the transmit power limit, regardless of the input channel conditions. This “constrained-by-design” architecture is a critical requirement for 6G regulatory compliance and network stability.

## IX. CONCLUSION

This paper presents Auto-Unrolled PGD, a framework integrating AutoGluon with deep-unfolded PGD for 6G beamforming. The expanded HPO search space—covering depth, step-size, optimizer, scheduler, layer type, and activation—enables autonomous discovery of both compact standard-PGD and richer hybrid architectures. A sum-loss training objective ensures batch-size-invariant gradients. Across  $N \in \{10^2, 10^3, 10^4, 5 \times 10^4\}$ , Auto-PGD consistently outperforms MLP, LISTA, and PGD-Net. At  $N = 10^3$ , it achieves 14.63 bits/s/Hz (98.8% of Classical PGD) with only 5 layers and a single forward pass—a  $40\times$  inference complexity reduction. Future work will extend this framework to massive MIMO and investigate robustness under imperfect CSI and hardware impairments.

## REFERENCES

- [1] Q. Hu, Y. Cai, Q. Shi, K. Xu, G. Yu, and Z. Ding, “Iterative algorithm induced deep-unfolding neural networks: Precoding design for multiuser mimo systems,” *IEEE Transactions on Wireless Communications*, vol. 20, no. 2, pp. 1394–1410, 2020.
- [2] A. Balatsoukas-Stimming and C. Studer, “Deep unfolding for communications systems: A survey and some new directions,” in *IEEE International Workshop on Signal Processing Systems (SiPS)*, 2019, pp. 266–271.
- [3] H. Liu and R. Foygel Barber, “Between hard and soft thresholding: optimal iterative thresholding algorithms,” *Information and Inference: A Journal of the IMA*, vol. 9, no. 4, pp. 899–933, 2019.
- [4] H. Huang, S. Guo, G. Gui, Z. Yang, J. Zhang, H. Sari, and F. Adachi, “Deep learning for physical-layer 5g wireless techniques: Opportunities, challenges and solutions,” *IEEE Wireless Communications*, vol. 27, no. 1, pp. 214–222, 2019.
- [5] M. Ibrahim, A. Mezghani, and E. Hossain, “Deep unfolding for sim-assisted multiband mu-miso downlink systems,” *arXiv preprint arXiv:2603.02122*, 2026.
- [6] A. T. Bui, R.-J. Reifert, H. Dahrouj, and A. Sezgin, “Deep unfolded fractional optimization for maximizing robust throughput in 6g networks,” *arXiv preprint arXiv:2602.06062*, 2026.
- [7] J. Zhu, T.-H. Chang, L. Xiang, and K. Shen, “Deepfpf: Deep-unfolded fractional programming for mimo beamforming,” *arXiv preprint arXiv:2601.02822*, 2026.
- [8] N. Shlezinger, S. Segarra, Y. Zhang, D. Avrahami, Z. Davidov, T. Rountenberg, and Y. C. Eldar, “Deep unfolding: Recent developments, theory, and design guidelines,” *arXiv preprint arXiv:2512.03768*, 2025.

- [9] N. Erickson, P. Larroy, H. Zhang, M. Li, A. Shirkov, J. Mueller, and A. Smola, "Autogluon-tabular: Robust and accurate automl for structured data," *arXiv preprint arXiv:2003.06505*, 2020. [Online]. Available: <https://arxiv.org/abs/2003.06505>
- [10] K. Filippou, G. Aifantis, G. A. Papakostas, and G. E. Tsekouras, "Structure learning and hyperparameter optimization using an automated machine learning (automl) pipeline," *Information*, vol. 14, no. 4, p. 232, 2023.
- [11] X. Wang and W. Zhu, "Advances in neural architecture search," *National Science Review*, vol. 11, no. 8, 2024.